VARIABLE STARS IN THE ULTRA-FAINT DWARF SPHEROIDAL GALAXY URSA MAJOR I[*]

Alessia Garofalo[1,2], Felice Cusano[2], Gisella Clementini[2], Vincenzo Ripepi[3], Massimo Dall'Ora[3],
Maria Ida Moretti[1,2,3], Giuseppina Coppola[3], Ilaria Musella[3], and Marcella Marconi[3]

[1] Dipartimento di Astronomia, Università di Bologna, Via Ranzani 1, I-40127 Bologna, Italy; alessia.garofalo@studio.unibo.it
[2] INAF-Osservatorio Astronomico di Bologna, Via Ranzani 1, I-40127 Bologna, Italy; fcusano@na.astro.it, gisella.clementini@oabo.inaf.it
[3] INAF-Osservatorio Astronomico di Capodimonte, Salita Moiariello 16, I-80131 Napoli, Italy; ripepi@na.astro.it, dallora@na.astro.it,
imoretti@na.astro.it, coppola@na.astro.it, ilaria@na.astro.it, marcella@na.astro.it

ABSTRACT

We have performed the first study of the variable star population of Ursa Major I (UMa I), an ultra-faint dwarf satellite recently discovered around the Milky Way (MW) by the Sloan Digital Sky Survey. Combining time series observations in the B and V bands from four different telescopes, we have identified seven RR Lyrae stars in UMa I, of which five are fundamental-mode (RRab) and two are first-overtone pulsators (RRc). Our V, $B - V$ color–magnitude diagram of UMa I reaches $V \sim 23$ mag (at a signal-to-noise ratio of ~ 6) and shows features typical of a single old stellar population. The mean pulsation period of the RRab stars $\langle P_{ab} \rangle = 0.628$, $\sigma = 0.071$ days (or $\langle P_{ab} \rangle = 0.599$, $\sigma = 0.032$ days, if V4, the longest period and brightest variable, is discarded) and the position on the period–amplitude diagram suggest an Oosterhoff-intermediate classification for the galaxy. The RR Lyrae stars trace the galaxy horizontal branch (HB) at an average apparent magnitude of $\langle V(RR) \rangle = 20.43 \pm 0.02$ mag (average on six stars and discarding V4), giving in turn a distance modulus for UMa I of $(m - M)_0 = 19.94 \pm 0.13$ mag, distance $d = 97.3^{+6.0}_{-5.7}$ kpc, in the scale where the distance modulus of the Large Magellanic Cloud is 18.5 ± 0.1 mag. Isodensity contours of UMa I red giants and HB stars (including the RR Lyrae stars identified in this study) show that the galaxy has an S-shaped structure, which is likely caused by the tidal interaction with the MW. Photometric metallicities were derived for six of the UMa I RR Lyrae stars from the parameters of the Fourier decomposition of the V-band light curves, leading to an average metal abundance of $[Fe/H] = -2.29$ dex ($\sigma = 0.06$ dex, average on six stars) on the Carretta et al. metallicity scale.

Key words: galaxies: dwarf – galaxies: individual (UMa I) – Local Group – stars: distances – stars: variables: RR Lyrae – techniques: photometric

Online-only material: color figures, machine-readable table

1. INTRODUCTION

The hierarchical theory of galaxy formation predicts that smaller galactic structures merge and dissolve to form the galaxies that we see today. Since 2004, 17 new dwarf companions have been discovered around the Milky Way (MW) from the analysis of the Sloan Digital Sky Survey (SDSS) data (see, e.g., Belokurov et al. 2007, 2010, and references therein). A similar number of new satellites have been discovered also around M31 (see, e.g., Richardson et al. 2011, and references therein). The new systems generally have luminosities fainter ($L_v \sim 10^3$–10^4 $L_\odot$; Belokurov et al. 2007) than the classical dwarf spheroidal (dSph) galaxies and have thus been named ultra-faint dwarfs (UFDs). They are usually dark matter dominated and spectroscopic analyses have revealed that they contain extremely metal-poor stars with metallicities as low as $[Fe/H] = -4.0$ dex (Tolstoy et al. 2009). In a number of cases they also show an irregular shape probably due to the tidal interactions with the MW. The UFD galaxies being discovered in large numbers around the MW and M31 galaxies are perhaps the best candidates for the lone survivors of the cannibalistic construction of the two giant spirals of the Local Group

(however, see Pawlowski et al. 2012a, 2012b, for challenges to the cosmological accretion scenario of galaxy formation).

The majority of the UFDs studied so far for variability have been found to contain pulsating variable stars of RR Lyrae type with pulsation characteristics (see, e.g., Clementini et al. 2012; Musella et al. 2012, and references therein) conforming to the properties of the variables in the MW globular clusters (GCs). In the MW the GCs that contain RR Lyrae stars divide into two different groups according to the mean period of the fundamental-mode (RRab) RR Lyrae stars (Oosterhoff 1939), and the number ratios of fundamental to first-overtone (RRc) pulsators ($f_c = N_c/N_{ab+c}$, where N_c and N_{ab} are the numbers of first-overtone and fundamental-mode RR Lyrae stars, respectively): Oosterhoff type I (OoI) clusters have $\langle P_{ab} \rangle \simeq 0.55$ days and $f_c \sim 0.17$, while Oosterhoff type II (OoII) GCs have $\langle P_{ab} \rangle \simeq 0.65$ days and $f_c \sim 0.44$ (Clement et al. 2001). Differences in the mean periods of the RRc stars are also found between the two groups, with the OoI GCs having RRc mean periods of ~ 0.32 days and the OoII GCs having mean periods of ~ 0.37 days (see, e.g., Catelan 2009). The Oosterhoff dichotomy is related to the metal content as OoII GCs are generally more metal-poor than the OoI GCs, but also the horizontal branch (HB) morphology plays an important role (Lee et al. 1990, 1999; Caputo et al. 2000). The Oosterhoff dichotomy is also present among the MW field RR Lyrae stars as first shown by Bono et al. (1997) and later confirmed by other studies (see, e.g., Miceli et al. 2008; Catelan 2009). The study of the Oosterhoff properties of the dwarf satellite companions of the

MW plays an important role in identifying which satellites may have been the building blocks of the Galactic halo. Indeed, the Oosterhoff dichotomy and the existence of an Oosterhoff gap have been observed so far only in the MW, as field and cluster RR Lyrae stars in the "bright" classical dSphs surrounding the MW have $0.58 \leqslant \langle P_{ab} \rangle \leqslant 0.62$ days and fall preferentially into the so-called Oosterhoff gap (Catelan 2009; Clementini 2010) avoided by the MW GCs.[4] Thus, the MW halo cannot have been assembled by accretion of dwarf galaxies resembling the present-day bright MW dSph satellites. On the contrary, the vast majority of the UFDs are found to contain RR Lyrae stars with OoII characteristics (see Clementini et al. 2012; Musella et al. 2012, and references therein), thus supporting the hypothesis that systems resembling the present-day UFDs might indeed have contributed to the building of the MW halo.

UMa I (R.A. $= 10^{h}34^{m}44^{s}$, decl. $= 51°55'33''.9$, J2000.0; $l = 160°$, $b = 54°$; Willman et al. 2005b) is, along with Willman 1 (Willman et al. 2005a), the first of the MW UFD satellites to be discovered by the SDSS. The galaxy has a half-light radius of $r_{h} = 11'.3 \pm 0'.5$ (Martin et al. 2008), which at the distance of 96.8 ± 4 kpc (Okamoto et al. 2008) corresponds to $r_{h} = 318^{+50}_{-39}$ pc. According to the absolute magnitude $M_{V} \sim -6.75$ mag estimated by Willman et al. (2005b), UMa I is about eight times less luminous than the faintest of the "bright" classical dSphs, namely, Draco, Sextans, and Ursa Minor. Based on a V, $V - I$ color–magnitude diagram (CMD) reaching $V \sim 25$ mag, Okamoto et al. (2008) conclude that UMa I contains an old stellar population comparable in age to the Galactic GCs M92 and M15. This was recently confirmed by Brown et al. (2012) whose much deeper CMD ($m_{F814W} \sim 28.5$ mag) obtained with the Advanced Camera for Surveys on board the *Hubble Space Telescope* (*HST*) shows the presence in UMa I of a single stellar population with an age of ~ 13.6 Gyr. Measuring the velocity dispersion of the brightest stars in UMa I, Kleyna et al. (2005) and Martin et al. (2008) found that the galaxy is one of the most dark matter dominated objects in the universe, with a mass-to-light ratio $M/L \sim 1000$ $M_{\odot}/L_{\odot}$. Simon & Geha (2007) confirmed the systemic velocity derived in these previous studies using a larger sample of stars, but derived a lower dispersion. Nevertheless, assuming the lower luminosity of UMa I ($M_{V} \sim -5.5$ mag) measured by Belokurov et al. (2006), Simon & Geha (2007) estimated an M/L similar to that of Kleyna et al. (2005) and Martin et al. (2008). In the same work Simon & Geha (2007) also derived a metal abundance of [Fe/H] $= -2.06 \pm 0.10$ dex from spectra of the galaxy red giants, later revised to [Fe/H] $= -2.29 \pm 0.04$ dex by Kirby et al. (2008), and to [Fe/H] $= -2.18 \pm 0.04$ dex by Kirby et al. (2011). UMa I appears to be strongly elongated (Martin et al. 2008), showing the signs of a possible tidal interaction with the MW (Okamoto et al. 2008).

In this paper, we present results from the study of the variable stars populating UMa I. The paper is organized as follows. Observations, data reduction, and calibration of the UMa I photometry are presented in Section 2. Results on the identification and characterization of the variable stars, the catalog of light curves, and the Oosterhoff classification are discussed in Section 3. The distance to UMa I and the metallicity of the RR Lyrae stars, derived from the Fourier analysis of the light curves, are presented in Section 4. The galaxy CMD is

Table 1
Log of the Observations

Telescope	Dates	Filter	N	Exposure Length (s)	FWHM (arcsec)
Cassini	2009 Feb 25–26	V	10	1500	2.5–3
	2009 Mar 23–25	V	11	1500	2.5–3
TLS	2009 Apr 19–25	B	21	900	2–2.2
	2009 May 18	B	17	900	2–2.2
	2009 Apr 19–25	V	24	1200	2–2.2
	2009 May 18	V	17	1200	2–2.2
TT1	2009 Nov 26	V	1	1500	2.5
	2010 Mar 20	V	3	1500	2.5
	2010 Mar 23	V	1	1500	2.5
Subaru	2005 Dec 31	V	5	10	0.6
	2006 Jan 1–3	V	24	10	0.7

discussed in Section 5 along with the spatial distribution of UMa I stellar components. Finally, a summary of the main results is presented in Section 6.

2. OBSERVATIONS AND DATA REDUCTIONS

Time series V, B photometry of UMa I was obtained in the period 2009–2010 at three different telescopes. The first set of V images was acquired using the Bologna Faint Object Spectrograph and Camera (BFOSC) mounted on the 1.52 m Cassini Telescope of the INAF-Bologna Observatory in Loiano.[5] BFOSC is a multipurpose instrument for imaging and spectroscopy, equipped with a 1340×1300 pixel EEV CCD with 0.58 arcsec pixel^{-1} scale. The total field of view (FOV) is of $12'.6 \times 13'$ and to fully cover the galaxy we needed two adjacent pointings. Observations of UMa I were performed in two nights in 2009 February, and in three nights in 2009 March, obtaining a total of 21 V images each with 1500 s exposure. The second set of 41 V images as well as 38 B exposures were obtained with the 2.0 m telescope at the Thueringer Landessternwarte Tautenburg (TLS)[6] equipped with a 2k × 2k SITe CCD at the Schmidt focus. The total FOV of the camera is $42' \times 42'$, with a pixel scale of 1.2 arcsec pixel^{-1}. Observations were performed in 2009 April and May. A third data set consisting of a few V images was obtained at the 1.54 m Toppo telescope TT1 of the Osservatorio Astronomico di Castelgrande[7] using the 2k × 2k SITe Toppo Telescope Scientific Camera (TTSC) which has a useful area of 2048×2048 pixels and a total FOV of $\sim 13' \times 13'$. These data were collected during one night in 2009 November and two nights in 2010 March. Finally, to increase the data sample and to enlarge the temporal baseline we complemented our photometry with V-band archive images of UMa I obtained with the Suprime-Cam at the Subaru Telescope (PI: N. Arimoto, ID proposals: o05167/o05223). These data were acquired during the nights from 2005 December 31 to 2006 January 3. The Suprime-Cam consists of a 5 × 2 array of 2048×4096 CCD detectors and provides a total FOV of $34' \times 27'$. The log of all the observations used in the present study is provided in Table 1.

Images were pre-reduced (bias-subtracted, trimmed, and flat-fielded) using standard routines within IRAF.[8] The PSF

Table 2
Identification and Properties of the RR Lyrae Stars Identified in UMa I

Name	α (2000)	δ (2000)	Type	P (days)	Epoch (max) HJD (-2454000)	$\langle B \rangle$ (mag)	$\langle V \rangle$ (mag)	A_B (mag)	A_V (mag)	[Fe/H] (a)	[Fe/H] (b)
V1	10:34:59.2	+51:57:07.3	RRab	0.56924	915.455	20.72	20.47	1.29	1.07	-2.16	-2.3 ± 0.2
V2	10:35:05.5	+51:55:39.8	RRab	0.584	886.660	20.85	20.37	1.09	0.78	...	...
V3	10:34:30.8	+51:56:28.9	RRab	0.64315	886.225	20.73	20.40	0.99	0.75	-2.17	-2.2 ± 0.3
V4	10:34:18.7	+51:58:29.2	RRab	0.74516	942.400	20.62	20.24	1.15	0.90	-2.30	-2.4 ± 0.2
V5	10:35:37.5	+52:02:35.6	RRab	0.59967	916.498	20.87	20.49	1.38	0.96	...	-2.3 ± 0.2
V6	10:33:07.1	+51:50:05.1	RRc	0.39673	886.980	20.73	20.42	0.72	0.63	...	-2.3 ± 0.1
V7	10:32:37.5	+51:49:55.7	RRc	0.40749	947.300	20.54	20.44	0.37	0.38	...	-2.2 ± 0.2

Notes.
(a) Metallicities from Kirby et al. (2008).
(b) Photometric metallicities from the Fourier parameters of the *V*-band light curve; they are on the Carretta et al. (2009) metallicity scale. Note that of the RRab stars only V5 fully satisfies the Jurcsik & Kovacs (1996) compatibility condition (see the text for details).

photometry was then performed using the DAOPHOT−ALLSTAR−ALLFRAME packages (Stetson 1987, 1994). The alignment of the images was performed using DAOMATCH, one of the routines in the DAOPHOT package, whereas DAOMASTER (Stetson 1992) was used to match the point sources. The *B* and *V* images were aligned using as a reference an image obtained at the TLS telescope, which has the largest FOV. This image was astrometrized using the WCStools available at http://tdc-www.harvard.edu/wcstools/, allowing us to astrometrize our catalogs. To perform the photometric calibration, as a first step, we cross-matched our photometric catalog with the SDSS catalog (Abazajian et al. 2009). From the SDSS catalog only objects flagged as stars and with good quality of the observations were selected. A total of 1118 stars were found to be in common between the two catalogs. The *g* and *r* magnitudes of the SDSS stars were first converted to standard Johnson *B* and *V* magnitudes using the calibration equations available at http://www.sdss.org/dr4/algorithms/sdssUBVRITransform.html. As a last step, the parameters of the photometric calibration were derived fitting the data to the equations $B_s - b = c_B + m_B \times (b-v)$ and $V_s - v = c_V + m_V \times (b-v)$, where B_s and V_s are the magnitudes of the SDSS stars in the Johnson system, and *b* and *v* are the magnitudes in our catalog. The fit was performed using a 3σ clipping rejection algorithm. A total of 581 stars were used in the final calibration, with magnitudes ranging from 15 to 23 mag in B_s and from -0.1 to 1.6 mag in $B_s - V_s$. The final rms of the fit is of 0.05 mag both in *B* and *V*. This accuracy is adequate for our main purpose of identifying the galaxy variable stars.

3. IDENTIFICATION OF THE VARIABLE STARS

Variable stars were identified on the *V, B* data separately, using the variability index computed in DAOMASTER (Stetson 1994). The signal-to-noise ratio (S/N) and the time coverage of the UMa I data are such that it allows the detection of variable stars as faint as $V \sim 22$ mag and $B \sim 22.5$ mag, and with periodicities in the range of a few hours to a few days for the *B* time series, and from a few hours to several days for the *V* data. A sample of 130 candidate variable stars were identified. Only candidate variables consistently varying in both passbands were retained. The *V, B* light curves of the candidate variables were analyzed with the Graphical Analyzer of Time Series (GRATIS), a private software developed at the Bologna Observatory by P. Montegriffo (see, e.g., Clementini et al. 2000) that first performs the period search using the Lomb periodogram (Lomb

Table 3
Johnson–Cousins *B, V* Photometry of UMa I Variable Stars

		Star V1—RRab			
HJD (-2454940)	B (mag)	err$_B$ (mag)	HJD (-2454940)	V (mag)	err$_V$ (mag)
1.33650	21.11	0.05	1.36133	20.79	0.04
1.39005	21.26	0.05	1.41162	20.96	0.06
1.43730	21.24	0.05	1.45850	20.85	0.06
1.46563	21.16	0.05	1.48730	20.76	0.05
2.35583	20.82	0.03	2.38037	20.50	0.04
2.39971	21.05	0.04	2.42432	20.62	0.05
2.43562	21.14	0.05	2.46143	20.64	0.04
3.33411	19.98	0.04	3.35889	19.88	0.05
3.40212	20.34	0.04	3.42725	20.19	0.06
3.43734	20.54	0.03	3.46191	20.33	0.06

(This table is available in its entirety in a machine-readable form in the online journal. A portion is shown here for guidance regarding its form and content.)

1976; Scargle 1982) and then the best fit of the data with a truncated Fourier series (Barning 1963). The final period adopted to fold the light curves was the one minimizing the rms scatter of the truncated Fourier series best fitting the data. We confirmed the variability and obtained reliable periods for seven variables in UMa I, all of RR Lyrae type. Five of them are fundamental-mode pulsators, while the remaining two are first-overtone variables. The identification and the properties of the RR Lyrae stars detected in UMa I are summarized in Table 2. We have assigned to the variables an increasing number starting from the galaxy center for which we adopted the coordinates by Martin et al. (2008). Column 1 gives the star identifier, Columns 2 and 3 provide the right ascension and declination (J2000 epoch), respectively. These coordinates were obtained from our astrometrized catalogs (see Section 2). Column 4 gives the type of RR Lyrae star, whether RRab or RRc, Columns 5 and 6 list the pulsation period and the Heliocentric Julian Day (HJD) of maximum light, respectively. With the only exception of the period for star V2 (see discussion below), all periods are accurate to the fifth digit. Columns 7 and 8 give the intensity-weighted mean *B* and *V* magnitudes, while Columns 9 and 10 list the corresponding amplitudes of the light variation. Finally, Columns 11 and 12 provide metallicities for some of the variable stars measured either spectroscopically or photometrically (see Section 4). The light curves of the variable stars are presented in Figure 1. The *B, V* time-series data of each variable star are provided in Table 3, which is published in its entirety in the electronic edition of the journal. Three of the RR Lyrae stars

identified in UMa I (namely, V1, V2, and V3) lie inside the galaxy half-light radius defined by Martin et al. (2008) (see Section 5). Stars V4, V5, and V6 lie slightly outside this region, but are still inside the galaxy radius. Finally, V7 is located at the edge of the FOV covered by our observations at a distance of 21ʹ.2 from the galaxy center. Star V2 is close to a very bright red ($B - V = 1.1$ mag) object, that significantly affects the star V magnitudes making it rather difficult to interpret the visual light curve (see Figure 1), whereas the B light curve appears to be only marginally affected. For this reason the period of V2 is less accurate than for the other six variables. Star V7 also has a scattered light curve. Its periodicity and the position on the HB (see Section 5) qualify V7 as a long period c-type RR Lyrae, but the star color, $B - V = 0.10$ mag, appears to be much bluer than the first-overtone blue edge of the RR Lyrae instability strip, for which the canonical value is $B - V \sim 0.18$ mag (see, e.g., Walker 1998). Further, the V-band amplitude of V7 is slightly larger than the B amplitude. The blue color of V7, the scatter in the light curve, and the reduced amplitude in the B band may be explained with the star being contaminated by a faint, blue, close companion. Finally, V4 is about 0.15–0.2 mag brighter than the other RR Lyrae stars; this along with the rather long period (0.75 days) may perhaps indicate that the star is evolved off the zero-age horizontal branch (ZAHB).

3.1. Bailey Diagram and Oosterhoff Classification

Figure 2 shows the V-band period–amplitude (Bailey) diagram of the UMa I RR Lyrae stars (filled triangles), according to the periods and V amplitudes reported in Table 2. We have also plotted in the figure the RR Lyrae stars identified in seven other UFDs: Coma (Musella et al. 2009), Leo IV (Moretti et al. 2009), Bootes I (Dall'Ora et al. 2006), CVn II (Greco et al. 2008), Hercules (Musella et al. 2012), UMa II (Dall'Ora et al. 2012), and Leo T (Clementini et al. 2012). The solid lines show the loci of the OoI and OoII Galactic GCs according to Clement & Rowe (2000). The position of the UMa I RR Lyrae stars in Figure 2 does not permit a firm classification of the galaxy in one of the two Oosterhoff groups. The average period of the five RRab stars in UMa I is $\langle P_{ab} \rangle = 0.628$ days ($\sigma = 0.071$ days, average on five stars). This value and the metallicity from Kirby et al. (2008, 2011) locate UMa I near the border between Oo-intermediate (Oo-Int) and OII objects in the [Fe/H]–$\langle P_{ab} \rangle$ plane (see, e.g., Figure 10 of Contreras Ramos et al. 2013). However, if we discard the longest period RRab variable (star V4, see Section 3) the average period becomes $\langle P_{ab} \rangle = 0.599$ days ($\sigma = 0.032$ days, average on four stars), and similarly if we only consider the RRab stars inside the galaxy half-light radius (V1, V2, and V3) we obtain $\langle P_{ab} \rangle = 0.599$ days ($\sigma = 0.039$ days, average on three stars) that definitely suggest an Oo-Int classification for UMa I.

4. METALLICITY AND DISTANCE TO UMa I FROM THE RR LYRAE STARS

An estimate of the metal abundance of the UMa I RR Lyrae stars can be obtained exploiting the relation existing between pulsation period and ϕ_{31} parameter of the Fourier decomposition of the V-band light curves (see Jurcsik & Kovacs 1996; Morgan et al. 2007, for a description of the method for RRab and RRc stars, respectively). Fourier parameters for the RR Lyrae stars we have identified in UMa I are provided in Table 4 along with the rms scatter (Column 11) of the Fourier best fit of the light curves. The last column of the table also provides values

Table 4
Parameters of the Fourier Decomposition of the V-band Light Curve

Star	Type	ϕ_{21}	errϕ_{21}	ϕ_{31}	errϕ_{31}	A_{21}	errA_{21}	A_{31}	errA_{31}	σ	D_m
V1	RRab	2.44	0.08	4.4	0.1	0.39	0.03	0.28	0.03	0.05	5
V2	RRab	2.6	0.2	5.3	0.6	0.44	0.09	0.18	0.07	0.1	11
V3	RRab	2.3	0.2	4.8	0.2	0.23	0.04	0.25	0.04	0.07	5
V4	RRab	2.28	0.08	5.06	0.09	0.52	0.04	0.45	0.04	0.05	6
V5	RRab	2.16	0.06	4.5	0.07	0.48	0.03	0.36	0.02	0.03	2.7
V6	RRc	2.8	0.2	5.6	0.5	0.29	0.05	0.12	0.05	0.06	(a)
V7	RRc	3.4	0.4	6.6	0.9	0.4	0.1	0.2	0.1	0.07	(a)

Notes. (a) The D_m value is defined only for RRab stars.

of D_m, a parameter measuring the regularity of the light curve for fundamental-mode RR Lyrae stars and setting the so-called compatibility condition, namely, $D_m < 3$, for a reliable application of the Jurcsik & Kovacs (1996) method to RRab stars. Of the UMa I fundamental-mode RR Lyrae stars only V5 has $D_m < 3$ (see Table 4). The metallicity of V5 derived with this technique is [Fe/H] $= -2.3 \pm 0.2$ dex, on the Carretta et al. (2009) metallicity scale (see Column 12 of Table 2). Among the other RRab stars V1, V3, and V4 do not strictly satisfy the Jurcsik & Kovacs (1996) compatibility condition, but are at the limit (V1 and V3) or slightly above (V4) the relaxed condition used in Cacciari et al. (2005) ($D_m < 5$), whereas V2 has a large D_m value definitely exceeding both Jurcsik & Kovacs (1996) and Cacciari et al. (2005) conditions. Since the Fourier fit of the light curves of V1, V3, and V4 appears to be very regular we still obtained an estimate of metallicity for these three stars, for which we find [Fe/H]$_{V1} = -2.3 \pm 0.2$ dex, [Fe/H]$_{V3} = -2.2 \pm 0.3$ dex, and [Fe/H]$_{V4} = -2.4 \pm 0.2$ dex. Our photometric metallicities are in very good agreement with the spectroscopic metallicity derived for V1, V3, and V4 by Kirby et al. (2008) (see Column 11 of Table 2). For the RRc stars we used the [Fe/H]–ϕ_{31}–P relations derived by Morgan et al. (2007) obtaining [Fe/H]$_{V6} = -2.3 \pm 0.1$ dex, and [Fe/H]$_{V7} = -2.2 \pm 0.2$ dex, on the Carretta et al. (2009) metallicity scale. The mean metallicity of the UMa I RR Lyrae stars derived from the Fourier parameters of the light curves is then [Fe/H] $= -2.29$ dex ($\sigma = 0.06$ dex, average on 6 stars), in excellent agreement with the mean metallicity of the UMa I red giants measured by Kirby et al. (2008) and only 0.1 dex lower than the revised value by Kirby et al. (2011).

The mean magnitude of the RR Lyrae stars, $\langle V(RR) \rangle$, can be used to derive the distance to UMa I. We find $\langle V(RR) \rangle = 20.40 \pm 0.08$ mag as the average over the seven stars. However, as discussed in Section 3, star V4 appears to be about 0.15–0.20 mag brighter than the other RR Lyrae stars and if, as we suspect, the star is evolved off the ZAHB it should not be used to estimate the galaxy distance. Furthermore, as UMa I appears to be rather elongated and structured (see Section 5), it may not be appropriate to average all together the RR Lyrae stars we have identified in the FOV of our observations to estimate the distance to the center of the galaxy. To have a better insight into this issue we computed the mean $\langle V(RR) \rangle$ value using different selections of the RR Lyrae and have summarized our results in Table 5. The different $\langle V(RR) \rangle$ estimates (see Column 2 of Table 5) agree within the errors and are all consistent with the V magnitude of the galaxy HB ($V(HB) = 20.45 \pm 0.02$ mag) derived by Okamoto et al. (2008), thus confirming the reliability of our absolute photometric calibration. However, the dispersion of $\langle V(RR) \rangle$ is significantly reduced if star V4 is discarded, therefore in the following we adopt the mean value
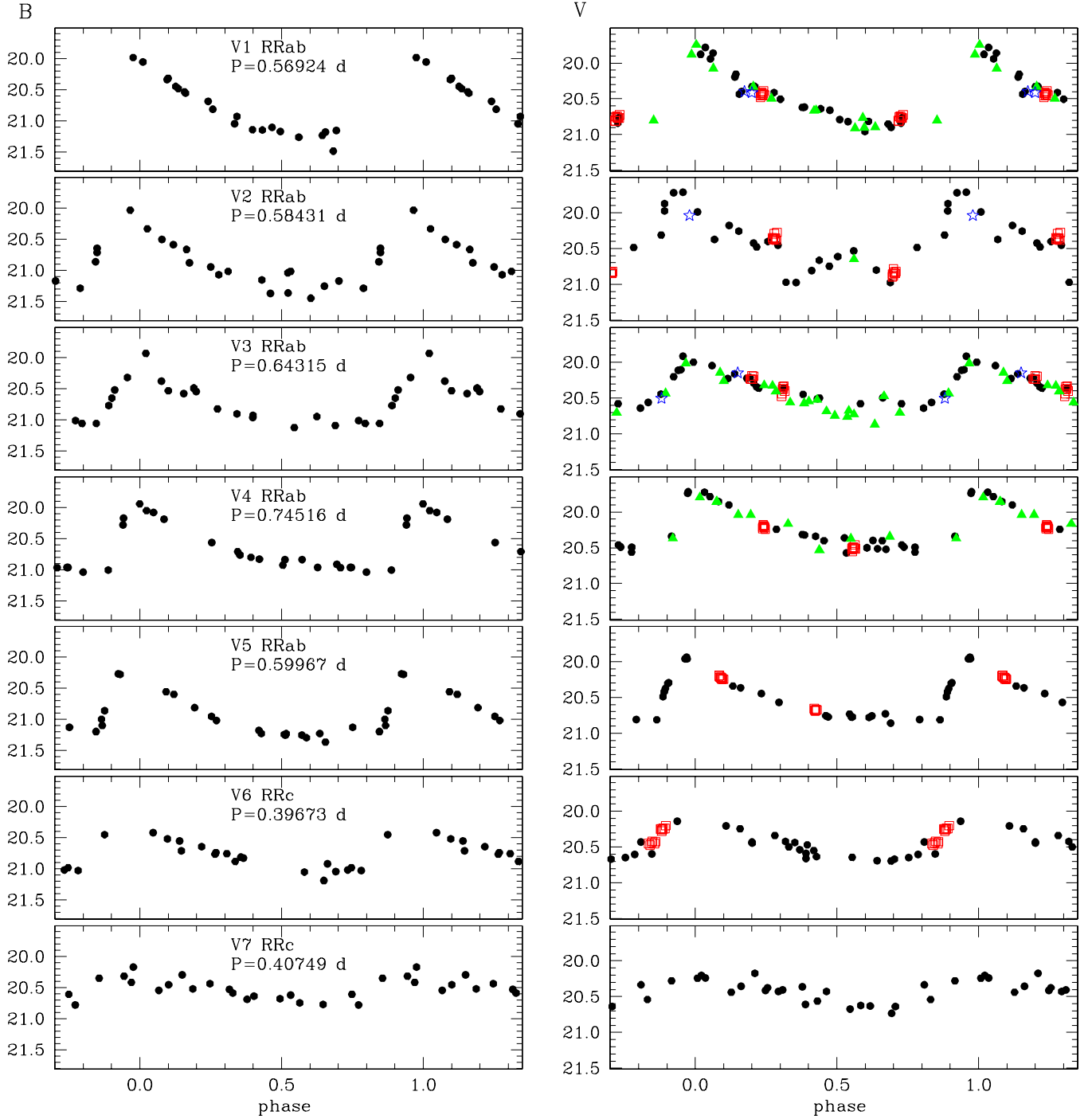
Figure 1. *B* (left panels) and *V* (right panels) light curves of the RR Lyrae stars we have identified in the UMa I galaxy. Black dots are TLS data, open (red) squares are SUBARU data, (green) triangles are Loiano data, and open (blue) stars are TT1 data.

(A color version of this figure is available in the online journal.)

Table 5
Average Magnitude of UMa I RR Lyrae Stars according to Different Sample Selections

Star's Selection	$\langle V(\mathrm{RR}) \rangle$ (mag)	σ (mag)	Notes
All	20.40 ± 0.03	0.08	
All minus V4	20.43 ± 0.02	0.04	
V1+V2+V3	20.41 ± 0.03	0.05	Only stars inside the r_h
V4+V5+V6+V7	20.40 ± 0.06	0.11	Only stars outside the r_h
V5+V6+V7	20.45 ± 0.04	0.03	Only stars outside the r_h and excluding V4
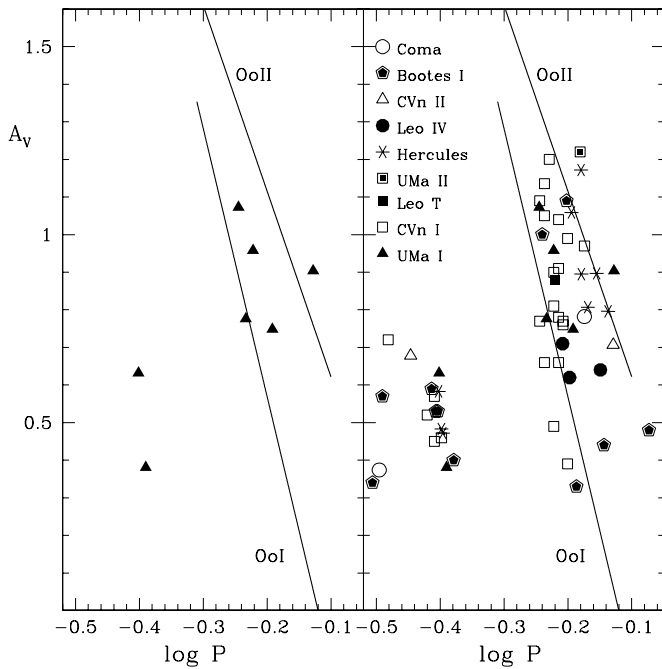
Figure 2. Left: V-band period–amplitude diagram of the RR Lyrae stars in UMa I; right: comparison with eight other UFDs studied for variability. In both panels, the solid lines show the loci of the OoI and OoII Galactic GCs from Clement & Rowe (2000).

obtained discarding star V4, $\langle V(RR)\rangle = 20.43 \pm 0.02$ mag, to estimate the distance to UMa I from the galaxy's RR Lyrae stars. We have also assumed $M_V = 0.54 \pm 0.09$ mag for the absolute visual magnitude of RR Lyrae stars with metallicity of [Fe/H] $= -1.5$ dex (Clementini et al. 2003) and $\Delta M_V/\Delta$[Fe/H] $= 0.214 \pm 0.047$ mag dex^{-1} (Clementini et al. 2003; Gratton et al. 2004) for the slope of the luminosity–metallicity relation of the RR Lyrae stars. For the galaxy's metallicity we have adopted the mean value we have derived from the RR Lyrae stars [Fe/H] $= -2.29 \pm 0.03$ dex. Schlegel et al. (1998) reddening maps give $E(B - V) = 0.019 \pm 0.026$ mag in the direction of UMa I, however, we obtain a slightly higher value of $E(B - V) = 0.04 \pm 0.02$ mag by fitting the galaxy CMD to the ridge lines of the Galactic GC M68 (see Section 5). This higher value is in excellent agreement with the reddening that Brown et al. (2012) obtain by fitting UMa I's RGB to the ridge line of the GC M92. In the following, we have thus assumed $E(B - V) = 0.04 \pm 0.02$ mag and the standard extinction law: $A_V = 3.1 \times E(B - V)$. The distance modulus of UMa I derived with this procedure is $\mu_0 = 19.94 \pm 0.13$ mag, corresponding to a distance $d = 97.3^{+6.0}_{-5.7}$ kpc, where the errors include the contribution of the uncertainties in the metallicity, reddening, photometry, photometric calibration, slope, and zero point of the M_V versus [Fe/H] relation, and on the average apparent visual magnitude of the UMa I RR Lyrae stars. Our distance modulus is in very good agreement with the distance modulus of $\mu_0 = 19.93 \pm 0.10$ mag, obtained by Okamoto et al. (2008) using the V magnitude of the HB estimated from the comparison with M92. Our value is also consistent, within the errors, with the distance modulus $\mu_0 = 19.99 \pm 0.04$ mag obtained for UMa I by Brown et al. (2012). Finally, we note that if we assume for the absolute visual magnitude of the RR Lyrae stars the brighter zero point by Benedict et al. (2011), $M_V = 0.45 \pm 0.05$ mag, for [Fe/H] $= -1.5$ dex, we obtain $\mu_0 = 20.03$ mag, which is respectively 0.10 mag and 0.04 mag longer than derived by Okamoto et al. (2008) and Brown et al. (2012).

5. CMD AND SPATIAL DISTRIBUTION OF UMa I MEMBER STARS

The V, $B - V$ CMD of UMa I obtained in this study is shown in Figure 3. We used the quality information provided by the DAOPHOT–ALLSTAR–ALLFRAME packages, namely, the ALLFRAME parameters χ and Sharp (see Stetson 1992), to clean the list of detected sources, selecting for the CMD only stellar detections with valid photometry on all input images, global Sharp parameter $-0.4 \leqslant$ Sharp $\leqslant 0.4$, and $\chi < 1.7$, in each filter. This allowed us to reduce the contamination by background galaxies. In the left panel of Figure 3 we have plotted all the stellar detections in the FOV of the TLS telescope, whereas in the middle panel we have reported only stars within the galaxy's half-light radius ($r_h = 11\rlap{.}'3$; Martin et al. 2008). Since UMa I is rather elongated, the radius used for the selection was defined by the equation $r^2 = x^2 + y^2/(1 - e)^2$, where e is UMa I's ellipticity for which we used $e = 0.80$ from Martin et al. (2008). Finally, the right panel shows instead objects in the TLS FOV that are located outside UMa I's half-light radius. In all panels, the RR Lyrae stars are marked by (red) open squares.

Typical internal errors of the combined photometry for non-variable stars at the magnitude level of UMa I HB ($V \sim 20.5$ mag) are $\sigma_V = 0.017$ mag and $\sigma_B = 0.026$ mag, respectively. The faintest stars in our CMD have $V \sim 23$ mag (at an S/N of ~ 6). In order to distinguish stars belonging to the UMa I galaxy from the overwhelming population of field stars belonging to the MW halo and disk we have cross-matched our photometric catalog against Simon & Geha (2007) and Kirby et al. (2008) catalogs of spectroscopically confirmed UMa I members. There are 32 stars in common between these catalogs; they are marked as (green) asterisks in Figure 3. Three of them are RR Lyrae stars identified in the present study, namely, stars V1, V3, and V4, whereas the remaining stars are mainly red giants. These stars along with the RR Lyrae variables allow to identify quite clearly UMa I's red giant and HBs. We have then overlaid on the CMDs in Figure 3 as (blue) solid lines the mean ridge lines of the Galactic GC M68 taken from Walker (1994). This cluster was selected because its metal abundance ([Fe/H]$_{M68} = -2.27 \pm 0.04$ dex; Carretta et al. 2009) well matches the metallicity of UMa I. The cluster ridge lines were shifted by +4.79 mag in V and -0.01 mag in $B - V$ to match the galaxy HB, the RR Lyrae stars, and the red giants with spectroscopically confirmed membership. These shifts imply a reddening $E(B - V) = 0.04 \pm 0.02$ mag for UMa I, in excellent agreement with Brown et al. (2012). The comparison with M68 confirms that UMa I, like M68, has a mostly old and metal-poor stellar population. The mean magnitude of the galaxy HB inferred from the match to M68 is $V = 20.45 \pm 0.11$ mag in excellent agreement with Okamoto et al. (2008), and very well consistent with the average magnitude of the RR Lyrae stars identified in this work, especially if the brightest and most likely evolved of our variables (star V4) is discarded.

Figure 4 shows a map of the stellar sources in the FOV of the TLS telescope that are in the CMD in the left panel of Figure 3. The (blue) ellipse is drawn using the half-light radius, the ellipticity, and the position angle of UMa I derived by Martin et al. (2008). Same as in Figure 3 the (green) asterisks are UMa I member stars spectroscopically confirmed by Kirby
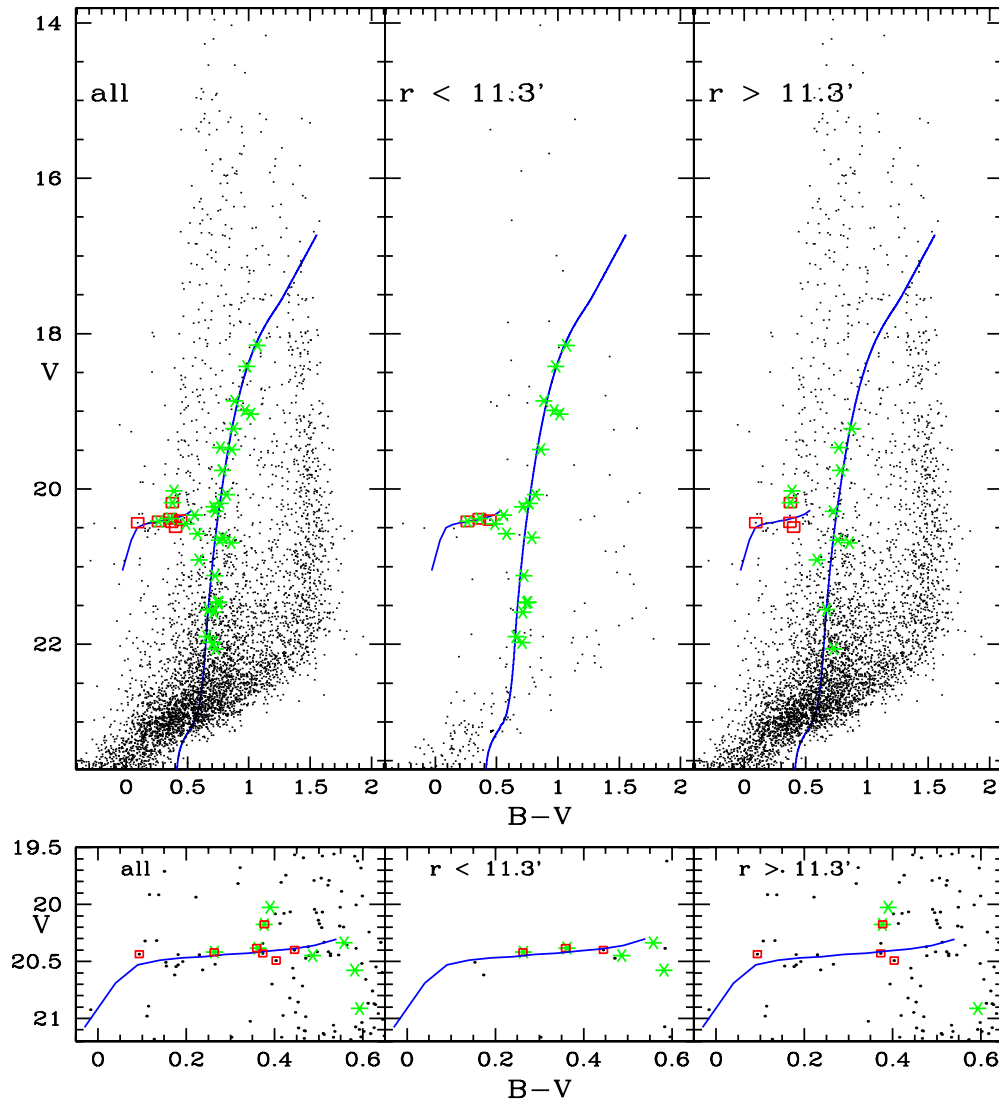
Figure 3. Upper panel, left: V, $B - V$ CMD of all the stellar detections in the FOV of the TLS telescope with valid photometry on all input images, global Sharp parameter $-0.4 \leqslant$ Sharp $\leqslant 0.4$, and $\chi < 1.7$, in each filter. The RR Lyrae stars are marked with (red) squares. Member stars of UMa I confirmed spectroscopically by Simon & Geha (2007) and Kirby et al. (2008) are marked with (green) asterisks. The (blue) solid line is the ridge line of the Galactic GC M68. Upper panel, middle: same as in the left panel, but for stars inside the half-light radius of UMa I. Upper panel, right: same as in the left panel, but for stars outside the galaxy half-light radius. Lower panels: zoomed-in view centered on the HB region of the CMDs shown in the upper panels.

(A color version of this figure is available in the online journal.)

et al. (2008) and Simon & Geha (2007), while the open (red) squares are the RR Lyrae identified in this work. The latter appear to be distributed along the galaxy major axis. In Figure 5, we show the isodensity map of RGB and HB stars selected from the CMD of UMa I (see Figure 3) by considering only stars within 0.1 mag from the ridge lines of M68. These stars were binned in $2'.4 \times 2'.4$ boxes and smoothed by a Gaussian kernel of FWHM of $2'.4$. The contours level are from 3σ above the background. The spectroscopically confirmed members of UMa I, the RR Lyrae stars, as well as the central isodensity contours appear to trace an S-shaped structure. This shape is a characteristic of dSph galaxies undergoing tidal stripping (e.g., HCC-087; Koch et al. 2012). In conclusion, both the high value of the ellipticity and the characteristic S-shaped structure of the stellar distribution suggest that UMa I is tidally interacting with the MW.

6. SUMMARY AND CONCLUSIONS

We have performed the first study of the variable stars in the UMa I UFD and detected seven RR Lyrae stars in the galaxy, of which five are RRab and two are RRc pulsators. Three of the RR Lyrae stars we have identified in UMa I were independently classified as member stars by Kirby et al. (2008) using medium-resolution spectroscopy. The average period of the five RRab stars is $\langle P_{ab} \rangle = 0.628$ days (or $\langle P_{ab} \rangle = 0.599$, if the brightest and longest period variable, star V4, is discarded) and suggests an Oo-Int classification for this UFD. UMa I is not the first of the new MW satellites to be classified as Oo-Int. The RR Lyrae stars identified in Canes Venatici I (CVn I; Kuehn et al. 2008) clearly have Oo-Int properties, and similarly, the lone RR Lyrae star identified in Leo T (Clementini et al. 2012) also suggests an
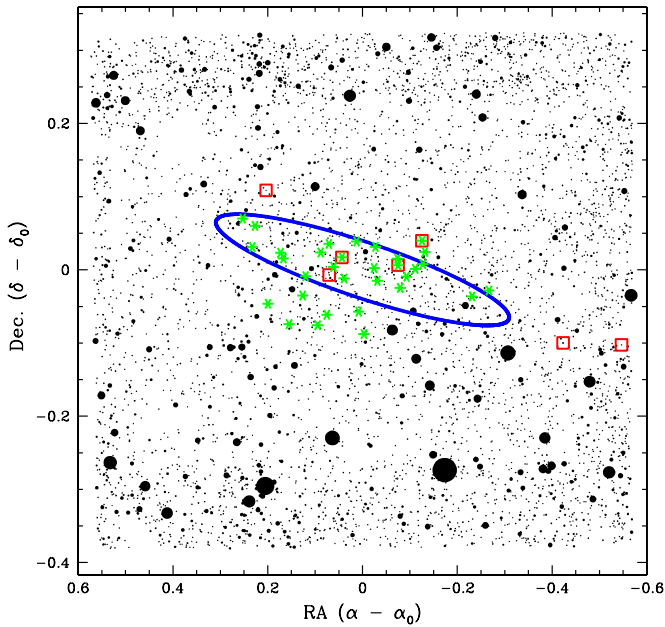
Figure 4. Map of all the sources in the FOV of the TLS telescope that we plot in the CMD in Figure 3. Symbol sizes are inversely proportional to the objects' magnitude. The (blue) ellipse traces the half-light radius region of UMa I, according to the position angle, half-light radius, ellipticity, and center coordinates (α_0, δ_0) of Martin et al. (2008). The (red) squares are the RR Lyrae identified in the present study. The (green) asterisks are UMa I members spectroscopically confirmed by Simon & Geha (2007) and Kirby et al. (2008).

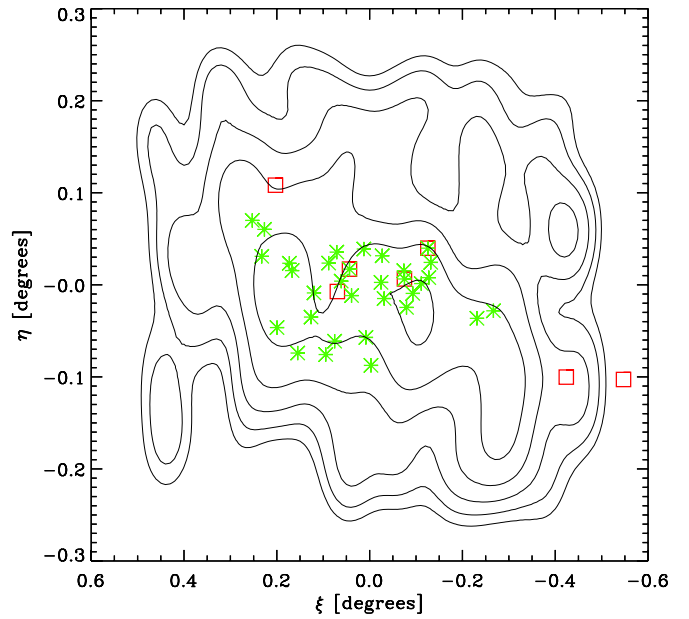(A color version of this figure is available in the online journal.)

Figure 5. Isodensity contours of UMa I RGB and HB stars selected from the galaxy CMD by considering only stars within 0.1 mag from the ridge lines of M68 (see the text for details). The plotted contour levels are from 3σ to 15σ above the background level. The (green) asterisks are UMa I members spectroscopically confirmed by Simon & Geha (2007) and Kirby et al. (2008); the (red) open squares are the RR Lyrae stars identified in this study.

(A color version of this figure is available in the online journal.)

Oo-Int classification for that UFD. However, both CVn I and Leo T have characteristics that set them apart from the "bona fide" MW UFDs. Specifically, CVn I is the brightest of the new MW satellites, and the high luminosity makes this galaxy much more similar to the classical dSphs than to the UFDs (see Figure 1 in Clementini et al. 2012). On the other hand, Leo T is the only UFD found to contain a significant amount of neutral gas and the lowest luminosity galaxy with ongoing star formation known to date. Hence, UMa I is so far the only "bona fide" UFD to exibit Oo-Int properties. The distance modulus of UMa I derived from the mean V magnitude of the RR Lyrae stars is $\mu_0 = 19.94 \pm 0.13$ mag, corresponding to $d = 97.3^{+6.0}_{-5.7}$ kpc. This distance is in good agreement with the estimates by Okamoto et al. (2008) and Brown et al. (2012). The individual metallicities derived for the RR Lyrae stars from the ϕ_{31} parameter of the Fourier decomposition of the light curve are in good agreement with the average spectroscopic metallicity derived for UMa I red giants by Kirby et al. (2008, 2011). The isodensity contours of red giants and HB stars properly selected from the galaxy CMD and the spatial distribution of both RR Lyrae stars and spectroscopically confirmed red giants (Simon & Geha 2007; Kirby et al. 2008) show that UMa I has an S-shaped structure, typical of dwarf galaxies undergoing tidal interaction.

REFERENCES

Abazajian, K. N., Adelman-McCarthy, J. K., Ageros, M. A., et al. 2009, ApJS, 182, 543
Barning, F. J. M. 1963, BAN, 17, 22
Belokurov, V., Walker, M. G., Evans, N. W., et al. 2010, ApJL, 712, L103
Belokurov, V., Zucker, D. B., Evans, N. W., et al. 2006, ApJL, 647, L111
Belokurov, V., Zucker, D. B., Evans, N. W., et al. 2007, ApJ, 654, 897
Benedict, G. F., McArthur, B. E., Feast, M. W., et al. 2011, AJ, 142, 187
Bono, G., Caputo, F., Cassisi, S., Incerpi, R., & Marconi, M. 1997, ApJ, 483, 811
Brown, M. T., Tumlinson, J., Geha, M., et al. 2012, ApJL, 753, L21
Cacciari, C., Corwin, T. M., & Carney, B. W. 2005, AJ, 129, 267
Caputo, F., Castellani, V., Marconi, M., & Ripepi, V. 2000, MNRAS, 316, 819
Carretta, E., Bragaglia, A., Gratton, R. G., et al. 2009, A&A, 505, 117
Catelan, M. 2009, Ap&SS, 320, 261
Clement, C. M., Muzzin, A., Dufton, Q., et al. 2001, AJ, 122, 2587
Clement, C. M., & Rowe, J. 2000, AJ, 120, 2579
Clementini, G. 2010, in Variable Stars, the Galactic Halo and Galaxy Formation, ed. N. Samus, C. Sterken, & L. Szabados (Moscow: Sternberg Astronomical Institute of Moscow Univ.), 107
Clementini, G., Cignoni, M., Contreras, R. R., et al. 2012, ApJ, 756, 108
Clementini, G., Di Tomaso, S., Di Fabrizio, L., et al. 2000, AJ, 120, 2054
Clementini, G., Gratton, R., Bragaglia, A., et al. 2003, AJ, 125, 1309
Contreras Ramos, R., Clementini, G., Federici, L., et al. 2013, ApJ, 765, 71
Dall'Ora, M., Clementini, G., Kinemuchi, K., et al. 2006, ApJL, 653, L109
Dall'Ora, M., Kinemuchi, K., Ripepi, V., et al. 2012, ApJ, 752, 42
Gratton, R. G., Bragaglia, A., Clementini, G., et al. 2004, A&A, 421, 937
Greco, C., Dall'Ora, M., Clementini, G., et al. 2008, ApJL, 675, L73
Jurcsik, J., & Kovacs, G. 1996, A&A, 312, 111
Kirby, E. N., Lanfranchi, G. A., Simon, J. D., et al. 2011, ApJ, 727, 78
Kirby, E. N., Simon, J. D., Geha, M., Guhathakurta, P., & Frebel, A. 2008, ApJL, 685, L43
Kleyna, J. T., Wilkinson, M. I., Evans, N. W., & Gilmore, G. 2005, ApJL, 630, L141
Koch, A., Burkert, A., Rich, R. M., et al. 2012, ApJL, 755, L13
Kuehn, C., Kinemuchi, K., Ripepi, V., et al. 2008, ApJL, 674, L81
Lee, J. W., & Carney, B. W. 1999, AJ, 117, 2868
Lee, Y. W., Demarque, P., & Zinn, R. 1990, ApJ, 350, 155
Lomb, N. R. 1976, Ap&SS, 39, 447
Martin, N. F., de Jong, J. T. A., & Rix, H.-W. 2008, ApJ, 684, 1075
Miceli, A., Rest, A., Stubbs, C. W., et al. 2008, ApJ, 678, 865

Moretti, M. I., Dall′Ora, M., Ripepi, V., et al. 2009, ApJL, 699, L125
Morgan, S. M., Wahl, J. N., & Wieckhorst, R. M. 2007, MNRAS, 374, 1421
Musella, I., Ripepi, V., Clementini, G., et al. 2009, ApJL, 695, L83
Musella, I., Ripepi, V., Marconi, M., et al. 2012, ApJ, 756, 121
Okamoto, S., Arimoto, N., Yamada, Y., & Onodera, M. 2008, A&A, 487, 103
Oosterhoff, P. T. 1939, Obs, 62, 104
Pawlowski, M. S., Kroupa, P., Angus, G., et al. 2012a, MNRAS, 424, 80
Pawlowski, M. S., Pflamm-Altenburg, J., & Kroupa, P. 2012b, MNRAS, 423, 1109
Richardson, J. C., Irwin, M. J., McConnachie, A. W., et al. 2011, ApJ, 732, 76

Scargle, J. D. 1982, ApJ, 263, 835
Schlegel, D. J., Finkbeiner, D. P., & Davis, M. 1998, ApJ, 500, 525
Simon, J. D., & Geha, M. 2007, ApJ, 670, 313
Stetson, P. B. 1987, PASP, 99, 191
Stetson, P. B. 1992, JRASC, 86, 71
Stetson, P. B. 1994, PASP, 106, 250
Tolstoy, E., Hill, V., & Tosi, M. 2009, ARA&A, 47, 371
Walker, A. R. 1994, AJ, 108, 555
Walker, A. R. 1998, AJ, 116, 220
Willman, B., Blanton, M. R., West, A. A., et al. 2005a, AJ, 129, 2692
Willman, B., Dalcanton, J. J., Martinez-Delgado, D., et al. 2005b, ApJL, 626, L85